Incorporation of Helium into Endohedral Complexes of C$_{60}$ and C$_{70}$ Containing Noble-Gas Atoms: A Tandem Mass Spectrometry Study

D. E. Giblin,[†] M. L. Gross,*,[†] M. Saunders,[‡] H. Jimenez-Vazquez,[‡] and R. J. Cross[‡]

*Contribution from the Departments of Chemistry, Washington University,
St. Louis, Missouri 63130, University of Nebraska, Lincoln, Nebraska 68588, and
Yale University, New Haven, Connecticut 06520*

Received April 7, 1997[⊗]

Abstract: Endohedral complexes of fullerenes and noble-gas atoms were originally prepared by a mass spectrometric method involving high-energy collisions of fullerene ions and noble-gas targets and, following that, by a high-pressure, high-temperature method involving neutral fullerenes and a noble gas as reactants. The latter method has made available sufficient quantities of the endohedral complexes of C$_{60}$ and C$_{70}$ with the various noble gases (He, Ne, Ar, and Kr) that the tandem mass spectrometric method can be used to test the possibility of preparing a new class of endohedral complexes that contain two noble-gas atoms. These new capture complexes do indeed form upon activation of the radical cation of the noble-gas endohedral complex by high-energy collisions with helium atoms. These complexes then decompose to give equivalent parallel losses of C$_2$ units accompanied by expulsion of none, one, or both of the captured noble-gas atoms. The capture event causes the gain in excess of 34 eV of additional internal energy, but the capture complexes survive on the time scale (∼50 µs) for the transit through the tandem mass spectrometer. Their survival, along with their fragmentation characteristics, is consistent with formation of an endohedral complex containing both noble-gas atoms although the fullerene cage may now be distorted especially when the fullerene is C$_{60}$. By analogy with the properties of empty fullerene and endohedral metallofullerene complexes, end points exist for the equivalent number of C$_2$ units that can be expelled to give a closed-structure product that contains either one or two noble-gas atoms. These end points correlate directly with the sizes of the fullerene and the noble-gas atom(s), giving support to our conclusion that endohedral complexes containing two noble gases can be prepared.

Introduction

One of the remarkable features of Buckministerfullerene, C$_{60}$, and related fullerenes is that their structures are closed cages with internal cavities large enough to accommodate atoms.[1] Shortly after their discovery, evidence for the formation of endohedral complexes of fullerenes with metals was reported.[2] The development of procedures to prepare bulk quantities of fullerenes[3] and endohedral metallofullerenes[4,5] facilitated studies on these materials. The metal is indeed inside the fullerene as has been demonstrated,[4,6,7] and for some species, the position of the metal is off-center,[8,9] which suggests bonding, not mere trapping.

Other characteristics of the fullerenes are their exceptional structural stability and the related features of self-assembly[10] and capacity for structural annealing and repair.[11,12] The primary pathway of dissociation of C$_{60}^{\bullet+}$ [13−16] and other fullerene radical ions,[17] as either metastable ions or following

collisional activation or photoactivation, is the equivalent loss of C$_2$ units. The same general pattern of fragmentation was reported for the endohedral metallofullerenes.[4,18] For both the empty and endohedral fullerenes, the loss of C$_2$ rather than the more stable C$_3$ has been taken as evidence of a closed structure.[17,18] A general feature of the fragment series corresponding to the equivalent loss of C$_2$ units is its abrupt termination, particularly after high-energy activation. (We refer

* Address correspondence to this author at Washington University.
† Washington University and University of Nebraska.
‡ Yale University.
⊗ Abstract published in *Advance ACS Abstracts,* October 1, 1997.
(1) Kroto, H. W.; Heath, J. R.; O'Brien, S. C.; Curl, R. F.; Smalley, R. E. *Nature* **1985**, *318*, 162−163.
(2) Heath, J. R.; O'Brien, S. C.; Zhang, Q.; Liu, Y.; Curl, R. F.; Kroto, H. W.; Tittel, F. K.; Smalley, R. E. *J. Am. Chem. Soc.* **1985**, *107*, 7779−7780.
(3) Krätschmer, W.; Lamb, L. D.; Fostiropoulos, K.; Huffman, D. R. *Nature* **1990**, *347*, 354−358.
(4) Chai, Y.; Guo, T.; Jin, C.; Haufler, R. E.; Chibante, L. P. F.; Fure, J.; Wang, L.; Alford, J. M.; Smalley, R. E. *J. Phys. Chem.* **1991**, *95*, 7564−7568.
(5) Johnson, R. D.; de Vries, M. S.; Salem, J.; Bethune, D. S.; Yannoni, C. S. *Nature* **1992**, *355*, 239−240.

(6) Bethune, D. S.; Johnson, R. D.; Salem, J. R.; de Vries, M. S.; Yannoni, C. S. *Nature* **1993**, *366*, 123−128.
(7) Beyers, R.; Kiang, C.-H.; Johnson, R. D.; Salem, J. R.; de Vries, M. S.; Yannoni, C. S.; Bethune, D. S.; Dorn, H. C.; Burbank, P.; Harich, K.; Stevenson, S. *Nature* **1994**, *370*, 196−199.
(8) (a) Hernández-Rojas, J.; Bretón, J.; Gomez Llorente, J. M. *J. Chem. Phys.* **1996**, *105*, 4482−4487. (b) Hernández-Rojas, J.; Bretón, J.; Gomez Llorente, J. M. *J. Chem. Phys.* **1996**, *104*, 5754−5760. (c) Hernández-Rojas, J.; Bretón, J.; Gomez Llorente, J. M. *J. Chem. Phys.* **1996**, *104*, 1179−1186.
(9) Tellgmann, R.; Krawez, N.; Lin, S.-H.; Hertel, I. V.; Campbell, E. E. B. *Nature* **1996**, *382*, 407−408.
(10) Smalley, R. E. *Acc. Chem. Res.* **1992**, *25*, 98−105.
(11) von Helden, G.; Gotts, N. G.; Bowers, M. T. *J. Am. Chem. Soc.* **1993**, *115*, 4363−4364.
(12) Hunter, J. M.; Fye, J. L.; Roskamp, E. J.; Jarrold, M. F. *J. Phys. Chem.* **1994**, *98*, 1810−1818.
(13) Foltin, M.; Lezius, M.; Scheier, P.; Märk, T. D. *J. Chem. Phys.* **1993**, *98*, 9624−9634.
(14) Hohmann, H.; Callegari, C.; Furrer, S.; Grosenick, D.; Campbell, E. E. B.; Hertel, I. V. *Phys. Rev. Lett.* **1994**, *73*, 1919−1922.
(15) Kolodney, E.; Tsipinyuk, B.; Budrevich, A. *J. Chem. Phys.* **1995**, *102*, 9263−9275.
(16) Laskin, J.; Lifshitz, C. *Int. J. Mass Spectrom. Ion Processes* **1994**, *138*, 95−106.
(17) O'Brien, S. C.; Heath, J. R.; Curl, R. F.; Smalley, R. E. *J. Chem. Phys.* **1988**, *88*, 220−230.
(18) Weiss, F. D.; Elkind, J. L.; O'Brien, S. C.; Curl, R. F.; Smalley, R. E. *J. Am. Chem. Soc.* **1988**, *110*, 4464−4465.

to the series of fragments separated by the mass of C_2 in this conventional manner, not as postulating a mechanism.) For empty fullerenes, such as $C_{60}^{\bullet+}$ and $C_{70}^{\bullet+}$, the series terminates at $C_{32}^{\bullet+}$,[17] whereas for certain endohedral metallofullerenes, the limiting sizes are $La@C_{44}^+$, $K@C_{44}^+$, and $Cs@C_{48}^+$.[2,18] These limits imply a minimum size for the fragments below which the closed structure is destroyed.[17,19] For the endohedral metallofullerenes, the evidence strongly implies that the metal is internal and that the contraction of the surrounding fullerene has in effect "shrink-wrapped" the metal.[4]

Lorents *et al.*[20] reported additional fragment series in a study employing very high-energy collisional activation. They produced product-ion spectra of the metallofullerene precursors, $Gd@C_{82}^+$ and $La@C_{82}^+$, by collisions with H_2, He, Ne, and Ar at laboratory kinetic energies of 80 and 160 keV. Series of fragments separated by C_2 loss start from $M@C_{82}^+$, $M@C_{82}^{2+}$, $C_{82}^{\bullet+}$, and C_{82}^{2+}. Furthermore, fragments MC_{2n}^+ and C_{2n+1}^+ form for $n < 12$. They could not determine the span of the various series because the mass resolving power of the instrument was insufficient.

Collisions of C_{60}, C_{70}, and C_{84}, in various charge states, with He, Ne, or Ar[21-24] or $Ne^{\bullet+}$ with C_{60}[25] at high energies in tandem-sector mass spectrometers were shown to form capture complexes. That these complexes are endohedral is supported by their survival on the time scale of these experiments even though the complexes contain >20 eV of internal energy, the acceptance of a second He atom by collision,[26] and persistence in neutralization—reionization experiments.[27] The amount of endohedral adduct formed in these mass spectrometric experiments, however, was insufficient for further studies of their properties. The high-energy insertion reactions have further implications for understanding collisional activations in tandem mass spectrometers where, under certain conditions, the projectile ion and target gas atom may not separate during high-energy, collisional activation.[28]

Saunders and collaborators developed a high-pressure method for preparing endohedral complexes of C_{60} and C_{70} with the noble gases, He, Ne, Ar, Kr, and Xe, and they verified the syntheses by mass spectrometry.[29] The method of synthesis

has made possible the production of macroscopic quantities of these interesting adducts.

We report research in this article that builds on the outcomes of the two methods for making noble-gas containing complexes and provides strong evidence that endohedral complexes of C_{60} containing the noble gases He, Ne, Ar, and Kr and of C_{70} containing Ne, Ar, and Kr can capture another atom. The results from studies of empty fullerenes and from a preliminary study involving $Kr@C_{60}^{\bullet+}$ [30] offer encouragement that collisional activation of the complexes would yield new complexes that contain two atoms and would lose C_2 units and/or the target gas atom. The extent of the loss of C_2 units, which is expected to be influenced by the endohedral components in a manner analogous to that of the "shrink-wrapped" metallofullerenes, is also a subject of this article. In addition, we consider whether collisional activation can cause the replacement of the endohedral gas atom by the target atom in addition to the formation of empty fullerenes. We expect that the exchange complexes will show fragments separated by C_2.

Experimental Section

All experiments were performed on a ZAB-T (Fisons, formerly VG, now Micromass, Wythenshawe, Manchester, UK), a four-sector tandem mass spectrometer of BEBE design where both the first stage mass spectrometer (MS1), B_1E_1, and the second stage (MS2), B_2E_2, are of double-focusing design.[31] The instrument was interfaced to a DEC VaxStation 3100 by the SIOS I interface supplied by the manufacturer. Instrument control and data collection and processing were controlled by the OPUS operating system, which was also supplied by the manufacturer.

The instrument was provided with four detectors: single-point detectors after B_1, MS1, and MS2, and a 15.2-cm (6-in.) array detector after MS2. The array detector offered significant improvement in the sensitivity of MS/MS experiments because it added multichannel advantage. Baseline resolving power, however, was degraded relative to half-height resolving power because photon "spreading" occurred in the phosphor element of the array detector.

Ions of the endohedral fullerenes were formed in an EI/CI source and mass selected at a resolving power of 1500—2000 in MS1. The source was operated in the EI mode with an electron-beam energy of 70 eV and an electron-beam current of $\sim$200 μA. The source operating temperature for these experiments was 400 °C. In addition, the source was baked out at the operating temperature for at least 4 h before the sample was introduced; this reduced the chemical background to a minimum. After each experiment, the source and probe were allowed to bake at temperature for 30—60 min before the next experiment to reduce sample carryover.

The complexes were placed in precut glass capillary tubes, which were in turn heated by the heated inlet probe to 400—630 °C as needed to maintain a steady signal intensity. Because there was a significant propensity of drawing electrical discharges at these operating temperatures, the heated probe was admitted to approximately 2 mm from the source, and the glass capillary tubes were cut to extend to the edge of the source without touching it.

All collisional activations (CA) were performed in the collision cell between MS1 and MS2. Gas pressure in the collision cell was adjusted to give a primary-ion beam suppression of approximately 60%. The collision gas was helium (^{4}He), and the precursor ions were accelerated to a kinetic energy of 8 keV. To distinguish between products that might arise by different paths, one of which would involve target capture, but produced the same nominal mass shift, ^{3}He was used as the collision gas for some experiments. For these experiments, the precursor ions were accelerated to a kinetic energy of 10 keV. This was done to keep the available collision energy, in the center-of-mass frame of reference, nearly constant (within $\sim$7%) for a given mass-

(19) von Helden, G.; Hsu, M.-T.; Gotts, N.; Bowers, M. T. *J. Phys. Chem.* **1993**, *97*, 8182—8192.

(20) Lorents, D. C.; Yu, D. J.; Brink, C.; Jensen, N.; Hvelplund, P. *Chem. Phys. Lett.* **1995**, *236*, 141—149.

(21) (a) Weiske, T.; Böhme, D. K.; Hrušák, J.; Krätschmer, W.; Schwarz, H. *Angew. Chem., Int. Ed. Engl.* **1991**, *30*, 884—886. (b) Weiske, T.; Böhme, D. K.; Schwarz, H. *J. Phys. Chem.* **1991**, *95*, 8451—8452. (c) Weiske, T.; Hrušák, J.; Böhme, D. K.; Schwarz, H. *Chem. Phys. Lett.* **1991**, *186*, 459—462. (d) Weiske, T.; Hrušák, J.; Böhme, D. K.; Schwarz, H. *Helv. Chim. Acta* **1992**, *75*, 79—89.

(22) (a) Caldwell, K. A.; Giblin, D. E.; Hsu, C. S.; Cox, D.; Gross, M. L. *J. Am. Chem. Soc.* **1991**, *113*, 8519—8521. (b) Caldwell, K. A.; Giblin, D. E.; Gross, M. L. *J. Am. Chem. Soc.* **1992**, *114*, 3743—3756.

(23) (a) Ross, M. M.; Callahan, J. H. *J. Phys. Chem.* **1991**, *95*, 5720—5723. (b) Mowrey, R. C.; Ross, M. M.; Callahan, J. H. *J. Phys. Chem.* **1992**, *96*, 4755—4761.

(24) (a) Campbell, E. E. B.; Ehlich, R.; Hielscher, A.; Frazao, J. M. A.; Hertel, I. V. *Z. Phys. D* **1992**, *23*, 1—2. (b) Kleiser, R.; Sprang, H.; Furrer, S.; Campbell, E. E. B. *Z. Phys. D* **1993**, *28*, 89—90.

(25) (a) Wan, Z.; Christian, J. F.; Anderson, S. L. *J. Chem. Phys.* **1992**, *96*, 3344—3347. (b) Christian, J. F.; Wan, Z.; Anderson, S. L. *J. Chem. Phys.* **1993**, *99*, 3468—3479.

(26) Weiske, T.; Schwarz, H. *Angew. Chem., Int. Ed. Engl.* **1992**, *31*, 605—606.

(27) (a) Weiske, T.; Wong, T.; Krätschmer, W.; Terlouw, J. K.; Schwarz, H. *Angew. Chem., Int. Ed. Engl.* **1992**, *31*, 183—185. (b) Wong, T.; Terlouw, J. K.; Weiske, T.; Schwarz, H. *Int. J. Mass Spectrom. Ion Processes* **1992**, *113*, R23—R29.

(28) Neumann, G. M.; Sheil, M. M.; Derrick, P. J. *Z. Naturforsch.* **1984**, *39a*, 584—592.

(29) Saunders, M.; Jiménez-Vázquez, H. A.; Cross, R. J.; Mroczkowski, S.; Gross, M. L.; Giblin, D. E.; Poreda, R. J. *J. Am. Chem. Soc.* **1994**, *116*, 2193—2194.

(30) Weiske, T.; Schwarz, H.; Giblin, D. E.; Gross, M. L. *Chem. Phys. Lett.* **1994**, *227*, 87—90.

(31) Gross, M. L. In *Methods in Enzymology*; McCloskey, J. A., Ed.; Acedemic Press: San Diego, 1991; Vol. 193, pp 131—153.

selected precursor.[32] (In this article, we prefer to consider the kinetic energy of the incident ions in the laboratory frame-of-reference unless otherwise noted.)

Product-ion spectra were obtained by scanning MS2 (such that $E_2/B_2 =$ constant) and collecting on the final single-point detector or by stepping MS2 and collecting multiple exposures per scan on the array, which was set at 15° relative to the main beam trajectory. Product-ion resolving power in both cases was typically 500−700. The choice of detector was made on the basis of the signal strength of the precursor ion beam. If possible, the single-point detector was used because it produces greater baseline resolving power than does the array detector.

Product-ion scans typically required a time of 30−60 s/scan. Scans were continually acquired as the sample was sublimed into the source chamber by heating the inlet probe. Typically, all usable scans from a run were summed together to achieve a spectrum with acceptable signal-to-noise ratios (see figures in the Results section).

The endohedral complexes containing noble gases were prepared by using the high-pressure synthetic procedure.[29] Each sample was a mixture of unreacted C$_{60}$ and C$_{70}$ with trace levels of endohedral complexes and other undetermined species. He@C$_{60}$ was prepared from a C$_{70}$-depleted stock of C$_{60}$; hence there was insufficient He@C$_{70}$ on which to perform experiments. The endohedral complexes were used without further purification.

Commercial prepurified helium, >99.9995% purity, was the source of ^{4}He. Helium-3 was purchased from EG&G Mound Applied Technologies (Miamisburg, OH) and had a stated purity >99.98%. Both gases were used as received.

Results

Considerations for Selection of Precursor Ion. We carried out tandem mass spectrometry experiments with the radical cations He@C$_{60}$$^{•+}$, Ne@C$_{60}$$^{•+}$, Ar@C$_{60}$$^{•+}$, Kr@C$_{60}$$^{•+}$, Ne@C$_{70}$$^{•+}$, Ar@C$_{70}$$^{•+}$, and Kr@C$_{70}$$^{•+}$ whose neutral precursors were present in the samples originally prepared by Saunders and co-workers.[29] C$_{60}$$^{•+}$ and C$_{70}$$^{•+}$ served as appropriate mass and abundance standards. The abundances of the endohedral complexes relative to their respective empty fullerenes were 0.4%, 0.2%, 0.3%, and 0.3% for the C$_{60}$ adducts that contain He, Ne, Ar, and Kr, respectively, and 0.2% for the three C$_{70}$ adducts. The abundance of Xe@C$_{60}$ relative to that of C$_{60}$ was approximately 0.008%, and the abundance of Xe@C$_{70}$ relative to C$_{70}$ was approximately 0.04% in the best preparation of the Xe-containing species, which were deemed too small to attempt MS/MS studies. The abundances of the various C$_{84}$ complexes were also too small to permit MS/MS studies. Furthermore, the overall abundance of C$_{70}$ relative to C$_{60}$ in the samples was about 15%. Because unreacted C$_{60}$$^{•+}$ was the most abundant species in the sample preparations, the synthetic C$_{60}$ and C$_{70}$ endohedral complexes represent ion abundances of ∼0.3% and ∼0.03% relative to the base species, C$_{60}$$^{•+}$. Because the abundances of the products were low, all spectra of the C$_{70}$ complexes were acquired by using the array detector, whereas either the single-point or the array detector was used for acquiring spectra of the C$_{60}$ complexes, depending on the precursor ion abundance.

The most abundant isotopic species in the molecular ion cluster (region) was mass-selected for all collisional activation studies. Because He and Ar are functionally monoisotopic and the most abundant isotope of Ne has the lowest mass, the base peaks in the isotope clusters were also the lowest in mass. Thus, the mass-selected Rg$_{base}$@^{12}C$_{60}$$^{•+}$ was essentially pure (no other isobaric species were present), and unless noted otherwise, Rg@C$_{60}$$^{•+}$ refers to that most abundant precursor. (Rg denotes any noble gas in an endohedral fullerene and Rg$_{base}$ is its most

---

(32) The available energy, T_A, is related to the laboratory kinetic energy, T_1, of the incident ion by $T_A = T_1 * m_T/(m_1 + m_T)$, where m_1 is the mass of the incident ion and m_T the mass of the target gas. See: Cooks, R. G. In *Collision Spectroscopy*; Cooks, R. G., Ed.; Plenum Press: New York, 1978; pp 1−16.
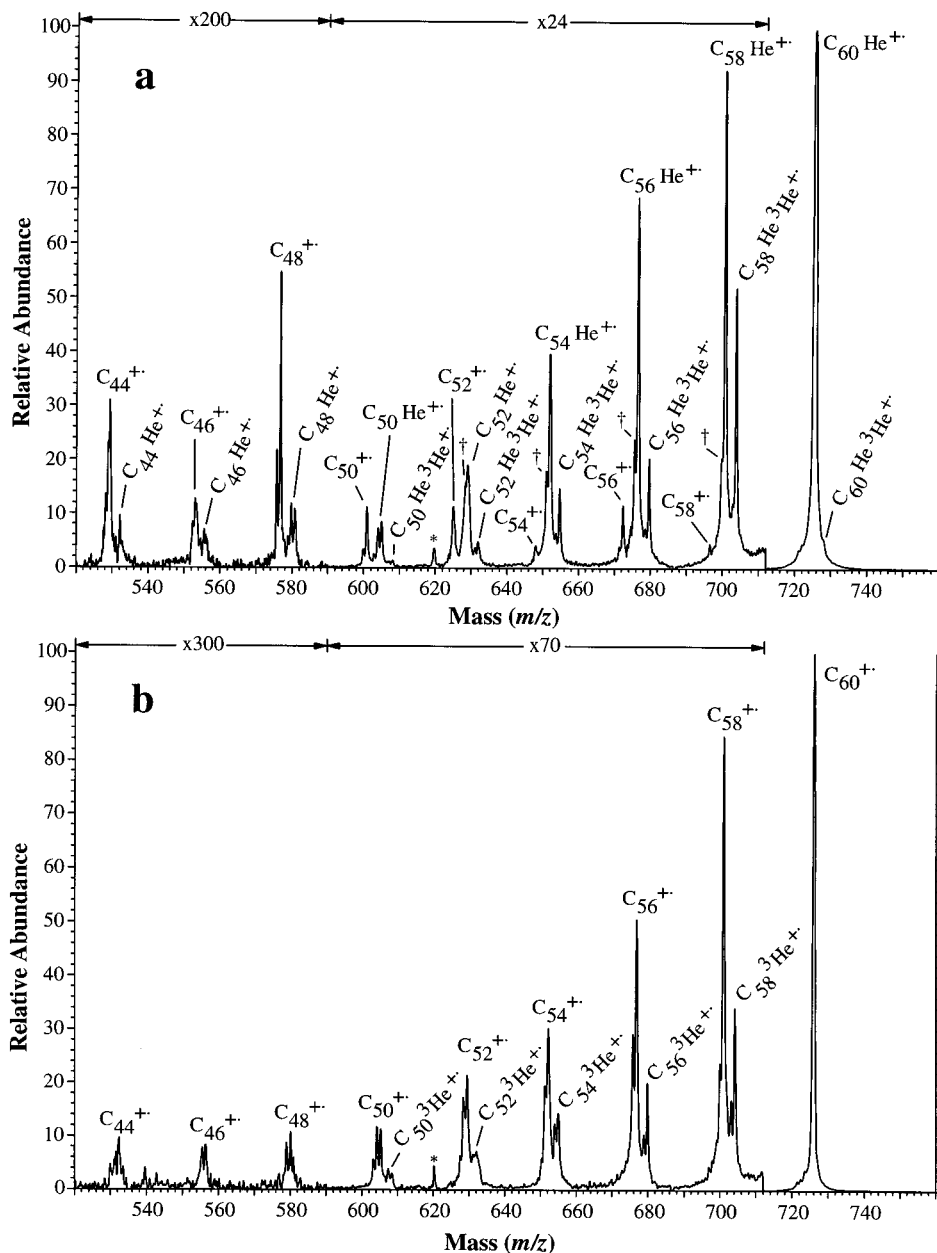
abundant isotope.) The most abundant species in the respective molecular ion regions for ^{84}Kr@^{12}C$_{60}$$^{•+}$ and ^{84}Kr@^{12}C$_{70}$$^{•+}$, however, suffer interferences from other isotopic species. In addition, the lowest-mass fullerene precursors containing ^{79}Kr or ^{81}Kr are essentially monoisotopic, but because the relative abundances, 0.5% and 3%, respectively, are low relative to the ^{84}Kr-containing species, it would be very difficult to obtain high-quality product-ion spectra of these monoisotopic species. At m/z 804, ^{83}Kr@^{13}C^{12}C$_{59}$$^{•+}$ and ^{82}Kr@^{13}C$_2$^{12}C$_{58}$$^{•+}$ occur with relative abundances of 13.7% and 4.5% with respect to ^{84}Kr@^{12}C$_{60}$$^{•+}$. Likewise, ^{83}Kr@^{13}C^{12}C$_{69}$$^{•+}$ and ^{82}Kr@^{13}C$_2$^{12}C$_{68}$$^{•+}$ have abundances of 15.9% and 6.2% relative to ^{84}Kr@^{12}C$_{70}$$^{•+}$ at m/z 924. The interferences have proven to be unimportant. (See Figure 4 and discussion later in this section.)

A consideration in the study of He@C$_{60}$$^{•+}$ is that, although the helium is functionally monoisotopic, there are severe interferences from the naturally occurring ^{13}C-containing isotopomers of the C$_{60}$$^{•+}$ cluster. At m/z 724, the abundance ratios of ^{13}C$_4$^{12}C$_{56}$/^{12}C$_{60}$ = 0.77%, whereas He@^{12}C$_{60}$/^{12}C$_{60}$ is approximately 0.4% giving He@^{12}C$_{60}$/^{13}C$_4$^{12}C$_{56}$ ∼ 0.5. But at m/z 725, ^{13}C$_5$^{12}C$_{55}$/^{12}C$_{60}$ = 0.10% and He@^{13}C^{12}C$_{59}$/^{12}C$_{60}$ ∼ 0.25%; therefore, He@^{13}C^{12}C$_{59}$/^{13}C$_4$^{12}C$_{56}$ ∼ 2.5. We expect the signal-to-background ratio to be five times better at m/z 725 than at m/z 724, where more of the information in the collisional activation decomposition (CAD) spectrum of He@^{12}C$_{60}$$^{•+}$ will be buried in the fragmentation of the non-endohedral species, here ^{13}C$_4$^{12}C$_{56}$$^{•+}$.

Another consideration in the study of He@C$_{60}$$^{•+}$ is whether collisional activation can cause the displacement of the captive endohedral helium with a target helium. If collisional activation is performed with ^{3}He as the target, exchange would give a collision product and a set of fragment ions that are one mass unit lower than those with the original ^{4}He.

Collisions of He@C$_{60}$$^{•+}$ with He. We chose to study He@C$_{60}$ by mass-selecting the ion of m/z 725, principally ^{4}He@^{13}C^{12}C$_{59}$$^{•+}$; the CAD spectrum is shown in Figure 1a. For comparison, Figure 1b is the CAD spectrum of C$_{60}$, without a captive helium and mass-selected as ^{13}C$_5$^{12}C$_{55}$$^{•+}$ at m/z 725. In both cases, the collision gas was ^{3}He, the kinetic energy was 10 keV, and the array detector was used. Note that the apparent abundances of the fragments of ^{13}C$_5$^{12}C$_{55}$$^{•+}$ decay more rapidly as m/z decreases than those of He@^{13}C^{12}C$_{59}$$^{•+}$ presumably due to greater isotopic splitting in the fragment clusters from ^{13}C$_5$^{12}C$_{55}$$^{•+}$ (*i.e.*, the probability for losing ^{13}C^{12}C and ^{13}C$_2$ *vs* ^{12}C$_2$ is higher for ^{13}C$_5$^{12}C$_{55}$$^{•+}$ than for He@^{13}C^{12}C$_{59}$$^{•+}$). That observation gives confidence that the fragments depicted and designated in the spectrum of He@^{13}C^{12}C$_{59}$$^{•+}$ originate predominantly from that species rather than from ^{13}C$_5$^{12}C$_{55}$$^{•+}$. The series of fragment ions that contain two helium atoms extends from He$_2$@C$_{60}$$^{•+}$ to He$_2$@C$_{50}$$^{•+}$. The series that contains one helium atom ends at He@C$_{44}$$^{•+}$, and the largest empty cage is C$_{58}$$^{•+}$. Other experiments in which the target was ^{4}He, the kinetic energy was 8 keV, and the single-point was the detector show additional species, He$_2$@C$_{48}$$^{•+}$, C$_{60}$$^{•+}$, and He@C$_{59}$$^{•+}$, in the CAD spectrum.

Product ions in which a target ^{3}He has displaced the initial endohedral ^{4}He during the course of fragmentation are manifest in the CAD spectrum (Figure 1a) of He@C$_{60}$$^{•+}$ by the splittings on the low-mass side of the peaks corresponding to fragments C$_{58}$He$^{•+}$, C$_{56}$He$^{•+}$, C$_{54}$He$^{•+}$, and C$_{52}$He$^{•+}$. Comparison of the same region of the CAD spectra taken of the two precursor ions of m/z 725 supports this identification because the relative abundances of the species at one mass lower are significantly greater in the CAD spectrum of He@C$_{60}$$^{•+}$ than in that of the isotopomer of C$_{60}$$^{•+}$ after relative gains are factored. The

Figure 1. Collisional activation mass spectra of mass-selected precursors at m/z 725 of (a) He@$C_{60}^{\bullet+}$ [He@$^{13}C^{12}C_{59}^{\bullet+}$] and (b) $C_{60}^{\bullet+}$ [$^{13}C_5^{12}C_{55}^{\bullet+}$]: (See Results.) In both cases, data acquisition employed the array detector, and the kinetic energy was 10 keV on a target of ^{3}He. The symbol † shows He exchange fragments (see Results) while * indicates artifacts of data collection on the array.

probability for the loss of ^{13}CC relative to loss of C_2 would be greater for the quintuple-^{13}C isotopomer of $C_{60}^{\bullet+}$ than for the mono-^{13}C isotopomer of He@$C_{60}^{\bullet+}$. The splittings of spectral peaks that correspond to product ions with a captured ^{3}He show the expected ratios due solely to isotopic probabilities.

The relative abundance of the fragments $C_{2n}{}^4He^{\bullet+}$ and $C_{2n}{}^3He^{\bullet+}$ in the CAD spectrum of He@$C_{60}^{\bullet+}$ with ^{3}He should be 1:1 in the absence of isotope effects if both He in the initially formed complex are endohedral and had randomized, and the fullerene cage had annealed prior to fragmentation. The ratio indicates preferential loss of ^{3}He, and the most likely explanation is that the fullerene cage had not yet fully annealed before the target ^{3}He departed through its entry port. The positions and energies of the two He atoms in the complex had not completely randomized before loss.

Collisions of Ne@$C_{60}^{\bullet+}$ and Ne@$C_{70}^{\bullet+}$ with He. Possible products that can form in the CAD of the Ne-containing endohedral complexes include fragments that have added He followed by loss of C_2 or those that simply expelled Ne; both

involve nominal losses of 20 u. To distinguish between these pathways, we subjected both Ne@$C_{60}^{\bullet+}$ and Ne@$C_{70}^{\bullet+}$ to collisional activation at 10 keV upon ^{3}He as target (the CAD spectrum of Ne@$C_{60}^{\bullet+}$ is shown in Figure 2a and that of Ne@$C_{70}^{\bullet+}$ is shown in Figure 2b; the inset in Figure 2a shows the congested and informative region of m/z 650–685).

For Ne@$C_{60}^{\bullet+}$, a series of product ions containing both Ne and He is formed, running from Ne^{3}He@$C_{60}^{\bullet+}$ to Ne^{3}He@$C_{52}^{\bullet+}$. Another series of fragments that contain only the original Ne is formed, terminating at Ne@$C_{44}^{\bullet+}$, and the largest empty cage is $C_{56}^{\bullet+}$. Note also the displacement fragment ions, ^{3}He@$C_{52}^{\bullet+}$ and ^{3}He@$C_{50}^{\bullet+}$, where the target ^{3}He has displaced the Ne in the complex. Although of low abundance, the existence of such ions is consistent with the observation that analogous fragments are produced for He@$C_{60}^{\bullet+}$.

For Ne@$C_{70}^{\bullet+}$, a series of product ions that contain both Ne and He is formed, running from Ne^{3}He@$C_{70}^{\bullet+}$ to Ne^{3}He@$C_{60}^{\bullet+}$, but of greater abundance than the corresponding series for Ne@$C_{60}^{\bullet+}$. A series of fragments containing the original Ne
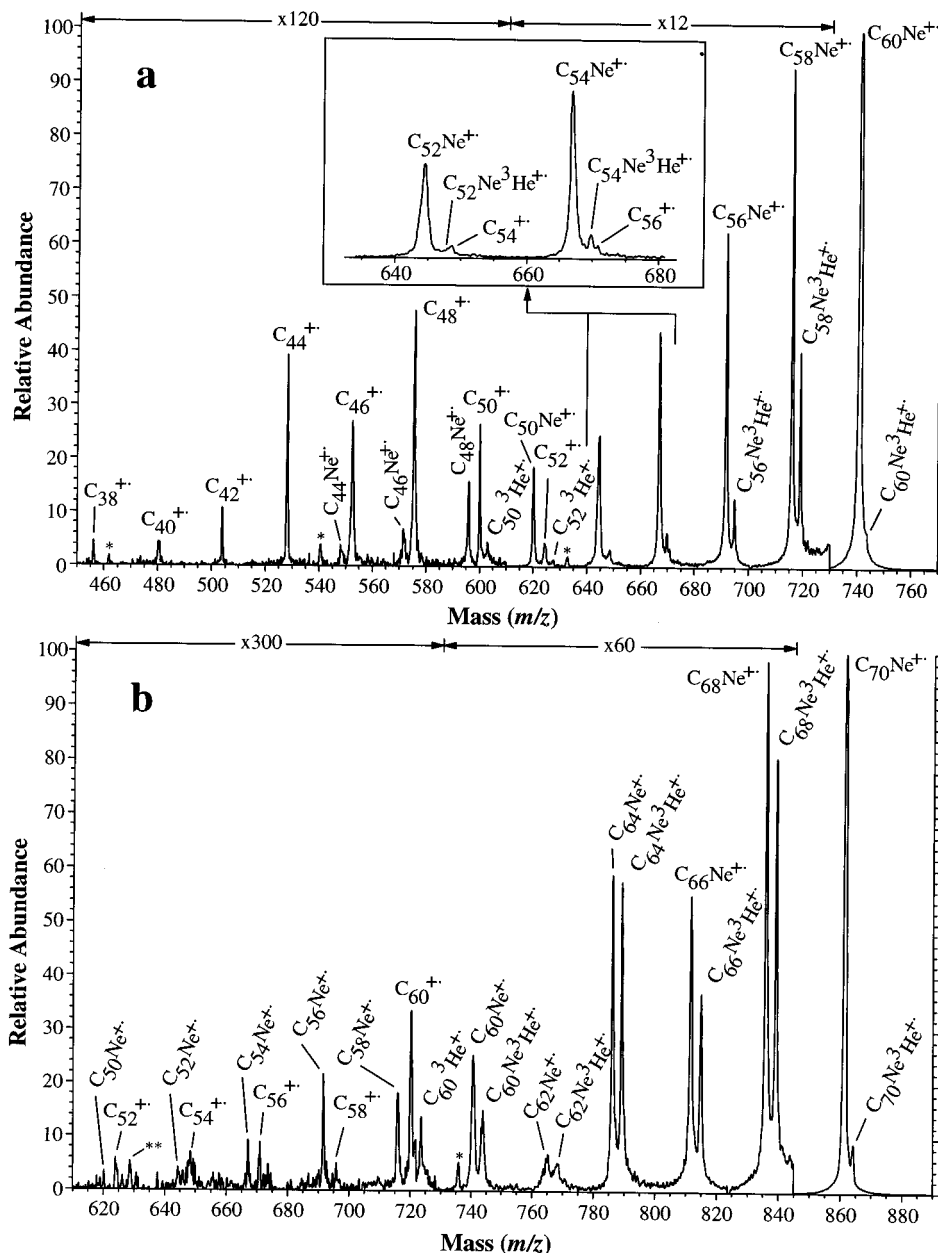
Figure 2. Collisional activation mass spectra of mass-selected (a) Ne@$C_{60}^{\bullet+}$, *m/z* 740, and (b) Ne@$C_{70}^{\bullet+}$, *m/z* 860. Inset on (a) magnifies the informative region of *m/z* 650−685. In both cases, data acquisition employed the array detector, and the kinetic energy was 10 keV on a target of ^{3}He. In part (a) the peaks for unknowns are indicated with an *, possibly artifacts from using the array, while in (b) the peaks are identified with an * for artifacts from using the array and ** for unknown.

is generated, terminating at Ne@$C_{50}^{\bullet+}$; and the largest empty cage is $C_{60}^{\bullet+}$. A displacement ion, ^{3}He@$C_{60}^{\bullet+}$, also is generated.

The abundances of the displacement ions with respect to their Ne-containing counterparts reveal that the captured ^{3}He is expelled in preference to the original Ne from the complexes initially formed upon CA.

Collisions of Ar@$C_{60}^{\bullet+}$ and Ar@$C_{70}^{\bullet+}$ with He. We collided Ar@$C_{60}^{\bullet+}$ and Ar@$C_{70}^{\bullet+}$ at 8 keV with He and were able to collect the CAD spectrum of the former by using the single-point detector and that of the latter by using the array detector. The CAD spectra for these complexes, shown in Figure 3a for Ar@$C_{60}^{\bullet+}$ and Figure 3b for Ar@$C_{70}^{\bullet+}$, present series of fragment ions that contain both Ar and He and span from ArHe@$C_{60}^{\bullet+}$ to ArHe@$C_{556}^{\bullet+}$ for Ar@$C_{60}^{\bullet+}$ and from ArHe@$C_{70}^{\bullet+}$ to ArHe@$C_{60}^{\bullet+}$ for Ar@$C_{70}^{\bullet+}$. The series of fragments that retain the original Ar terminate at Ar@$C_{46}^{\bullet+}$ and Ar@$C_{54}^{\bullet+}$ for Ar@$C_{60}^{\bullet+}$ and Ar@$C_{70}^{\bullet+}$, respectively. For

Ar@$C_{60}^{\bullet+}$, the series of carbon-only fragments extends downward from $C_{54}^{\bullet+}$, whereas for Ar@$C_{70}^{\bullet+}$, there is only the single species $C_{60}^{\bullet+}$. Presumably these are empty fullerene cages.

When both Ar-containing precursor ions are mass-selected for CA, fullerene-like contaminants of the same nominal mass appear to be co-selected, and they fragment upon CA to lose 36 and 40 u. Although such losses appear to mimic the processes of helium uptake coupled with Ar loss or simple Ar loss, their time profile during probe heating was different than those of the other fragments in the spectra.

Collisions of Kr@$C_{60}^{\bullet+}$ and Kr@$C_{70}^{\bullet+}$ with He. We activated Kr@$C_{60}^{\bullet+}$ and Kr@$C_{70}^{\bullet+}$ at 8 keV by collision with He (see Figure 4, parts a and b, for the CAD spectra of Kr@$C_{60}^{\bullet+}$ and Kr@$C_{70}^{\bullet+}$, respectively). The single-point detector was employed for Kr@$C_{60}^{\bullet+}$ whereas the array detector was needed for Kr@$C_{70}^{\bullet+}$. The effects of isotopic interferences in ^{84}Kr@$^{12}C_{60}^{\bullet+}$ and ^{84}Kr@$^{12}C_{70}^{\bullet+}$ that were coselected for MS/MS (see earlier discussion in this section) are manifest by minor
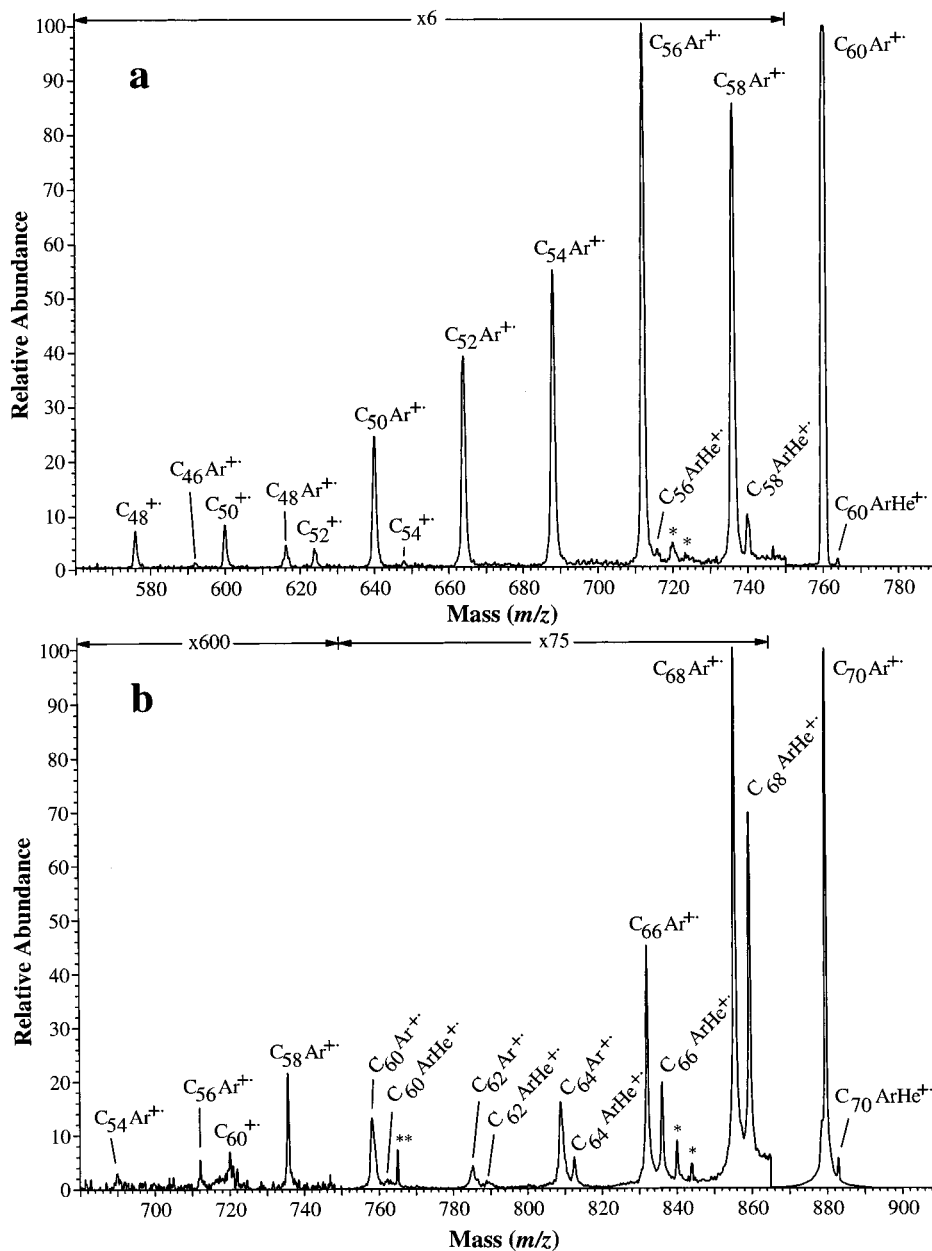
Figure 3. Collisional activation mass spectra of mass-selected (a) Ar@$C_{60}^{\bullet+}$, *m/z* 760, and (b) Ar@$C_{70}^{\bullet+}$, *m/z* 880. For part (a), data acquisition used the single-point detector, and the kinetic energy was 8 keV on a target of ^{4}He. For part (b), data acquisition used the array detector, and the kinetic energy was 8 keV on a target of ^{4}He. In both spectra, the * marks apparent chemical artifacts. (See Results.) In part (b), the ** indicates the artifact from using the array.

broadening around the base of the peaks in the spectra and are minor, as was previously reported for Kr@$C_{60}^{\bullet+}$.[30] For the spectrum of ^{84}Kr@$^{12}C_{70}^{\bullet+}$, physical effects in the array detector broaden the peaks to a greater extent than do isotopes.

For Kr@$C_{60}^{\bullet+}$, the only fragments containing both Kr and He are KrHe@$C_{60}^{\bullet+}$ and KrHe@$C_{58}^{\bullet+}$. The series of fragments containing only Kr terminates at Kr@$C_{48}^{\bullet+}$. The series of empty fragments starts at $C_{54}^{\bullet+}$ and runs downward. We were not able to reproduce, in several repeated experiments, a peak indicating the presence of $C_{60}^{\bullet+}$ among the fragments generated from Kr@$C_{60}^{\bullet+}$, otherwise, these results agree with those published earlier,[30] even though there are differences of kinetic energies.[33]

For Kr@$C_{70}^{\bullet+}$, the series of fragments that contain both noble-gas atoms is present from KrHe@$C_{70}^{\bullet+}$ to KrHe@$C_{64}^{\bullet+}$. The

series of fragments that contain only Kr persists down to Kr@$C_{56}^{\bullet+}$. Unlike the other systems discussed above, there were no detectable, empty fragments derived from this precursor. It is possible that while collisions can transiently open a cage, the rend created with the collision energies available in these experiments may not be sufficiently large to permit the escape of the large Kr atom.

Discussion

Fullerene radical cations $C_{60}^{\bullet+}$ formed by electron ionization at 70 eV acquire substantial internal energy during the formation process, up to ~45 eV.[13] It is expected that the primary ions of the endohedral complexes would carry similar ranges of internal energies into the collisional activation events.

All collision activation experiments in this study were carried out by suppressing the precursor ion beam by ~60%, the level at which the probabilities of single-, double-, and triple-collision

(33) (a) Moseley, J. A.; Cooper, H. J.; Gallagher, R. T.; Derrick, P. J. *Eur. J. Mass. Spectrom.* **1995**, *1*, 501−502. (b) Moseley, J. A.; Gallagher, R. T.; Derrick, P. J. *Proceedings: 44th ASMS Conference on Mass Spectrometry and Allied Topics*; Portland, Oregon, 1996; p 1251.
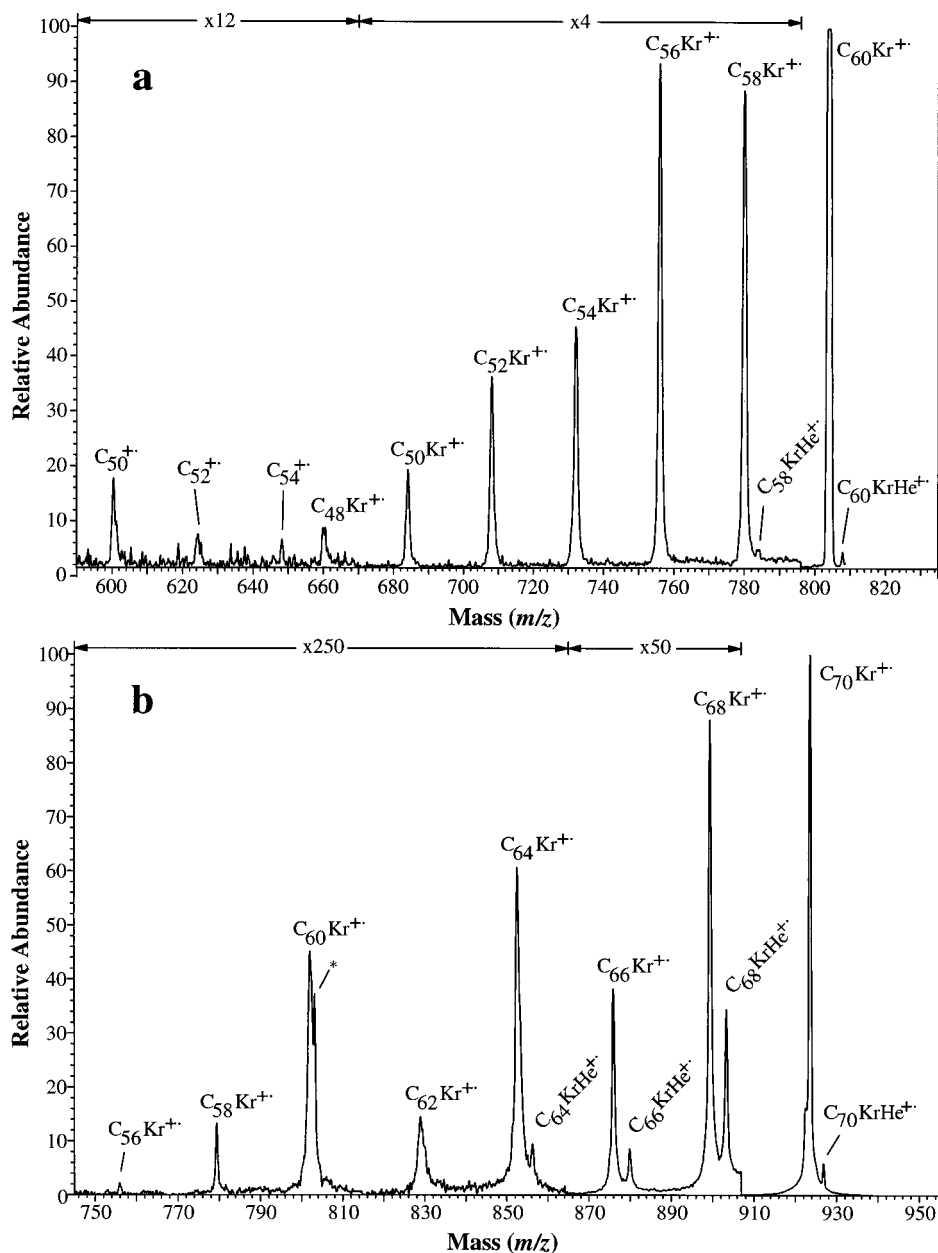
Figure 4. Collisional activation mass spectra of mass-selected (a) Kr@$C_{60}^{\bullet+}$, *m/z* 804, and (b) Kr@$C_{70}^{\bullet+}$, *m/z* 924. For part (a), data acquisition used the single-point detector, and the kinetic energy was 8 keV on a target of ^{4}He. For part (b), data acquisition used the array detector, and the kinetic energy was 8 keV on a target of ^{4}He.

events are 21%, 26%, and 21%, respectively.[34] Although the probability of multiple collisions within the collision cell is predominant, most of the fragmentations and target capture are driven by energy acquired by a large impact parameter collision with the target gas.[22a,25b,28] The precursor ions in this study can acquire internal energies from a capture-event collision that are in excess of 34 eV. The transit time through the collision cell and accompanying drift region is ∼1.5 μs, and all fragments must be formed during this time to be transmitted to the detector. Furthermore, the fragments, once formed, must be sufficiently stable that some fraction of the population survives the transit time, ∼50 μs, through the second stage (MS2) of the tandem mass spectrometer. Some precursor ions of C_{60} or C_{70} which

are formed by 70 eV electron ionization and are subjected to multiple-collision conditions may acquire internal energies in excess of 90 eV, which could drive ≥7 steps of sequential C_2 losses or equivalent[13] during the transit time. Because the interaction between the noble gas and the surrounding fullerene is van der Waals, it is expected that the maximum energies attained during formation and activation of the noble-gas endohedral complexes would be similar to those for $C_{60}^{\bullet+}$ or $C_{70}^{\bullet+}$, and fragmentation would be driven similarly.[35]

The experimental results (see Table 1) show that activation of the noble-gas endohedral complexes by collisions with He results in the formation of complexes that contain both the original noble-gas atom and the target He atom. These complexes, along with those that contain only the original noble-gas atom, fragment to produce series of fragment ions that are

(34) Collision probabilities were calculated according to a literature procedure (Kim, M. S. *Int. J. Mass Spectrom. Ion Processes* **1983**, *50*, 189–203, with modifications to account for the main beam being composed of uncollided and collision survivor ions. The relative collision cross sections were derived from MIKES data in ref 22b. Details of the differences of collision probabilities vs beam suppression between MIKES and double-focusing instruments are the subject of a future publication.

(35) Laskin, J.; Jiménez-Vázquez, H. A.; Shimshi, R.; Saunders, M.; de Vries, M. S.; Lifshitz, C. *Chem. Phys. Lett.* **1995**, *242*, 249–252.

(36) Emsley, J. *The Elements*, 2nd ed.; Clarendon Press, Oxford, 1991.

Table 1.   End Points of Observed Series of Fragments in the CAD Spectra

precursor[a] $M^{•+}$	radii[b]	target[c]	T_A[d], eV	series termini: max n[e]			other products
				$(M - nC_2)^{•+}$	$(M - nC_2 + He)^{•+}$	$C_{2n}^{•+}$	
$C_{60}^{•+}$ [f]		^4He	44.2	12	8		$C_{59}^{•+}$
$He@C_{60}^{•+}$	1.22	^3He	41.1	8[g]	6	30	$C_{59}He^{•+}$
							$C_{58}He^{•+}, C_{56}He^{•+}, C_{54}He^{•+}, C_{52}He^{•+}$
$Ne@C_{60}^{•+}$	1.60	^3He	40.4	8	4	28	$C_{52}He^{•+}, C_{50}He^{•+}$
$Ar@C_{60}^{•+}$	1.91	^4He	41.2	7	2	27	
$Kr@C_{60}^{•+}$	1.98	^4He	39.6	6	1	27	
$C_{70}^{•+}$ [f]		^3He	35.6	>10	10		
$Ne@C_{70}^{•+}$	1.60	^3He	34.8	10	5[h]	30	$C_{60}He^{•+}$
$Ar@C_{70}^{•+}$	1.91	^4He	36.8	8	5	30	
$Kr@C_{70}^{•+}$	1.98	^4He	34.5	7	3	h	

[a] CAD spectra of $C_{60}^{•+}$ and $C_{70}^{•+}$ not presented but consistent with published data. [b] Radii: Van der Waals radii of the noble gases in the endohedral complexes.[36] [c] Target: gas used as the target for collisional activation. [d] T_A, eV: available collision energy (center-of-mass).[32] [e] Max n: $(M - nC_2)^{•+}$ and $(M - nC_2 + He)^{•+}$: smallest member of a fragment series observed. $C_{2n}^{•+}$: largest member of a series observed. [f] Precursor, $M^{•+}$: species that is mass selected for collisional activation. [g] Limited by chemical background. [h] Limited by signal/noise.

separated by the mass of C_2. The results are analogous to those for the activation of empty fullerenes by collisions with He.[21–24]

During capture, all the available (center-of-mass) collision energy, T_A, is converted to internal energy of the complex,[22b] which in conjunction with preexisting internal energy and that from other collision processes drives the fragmentation processes including ejection of the captured He atom. Experimental evidence that we presented in an earlier study of $C_{60}^{•+}$ fragmentation indicates that $C_{58}^{•+}$ originates from $He@C_{60}^{•+}$.[22a] But other results also indicate that efficient methods of activation (*e.g.*, photoionization[17] and non-capture collisional activation, such as by Xe[22b]) also drive the C_2 fragmentation.

In this study, the maximum internal energy gain that is available from a capture-event or large impact parameter collisions is greater than 34 eV. The existence of precursor ions that have captured a target He atom provides strong evidence that both the original endohedral component and the He target gas are internal. An externally bound He, held only by van der Waals forces, would detach more readily from the activated complexes than would C_2 units. Furthermore, the fragments formed by loss of C_2 units from the original capture complexes are evidence that both gas atoms are endohedral. A third line of evidence, the extent of the fragment ion series (loss of C_2) that originate from the various capture complexes, represents the most dramatic trend in Table 1. The span of this fragment ion series is inversely dependent upon the size (*i.e.*, van der Waal radius) of the initial endohedral component, which suggests that the resulting product ion series are approaching the limits of closed structural integrity ("shrink-wrapping"), although the geometry of these complexes may be significantly distorted. The analogous C_{70} complexes show a similar but less pronounced trend whereby the smallest species observed for each initial capture complex are larger than the corresponding ones seen for the C_{60} complexes. The C_{70} complexes receive approximately 4 eV less activation energy from the capture of the target than do the C_{60} complexes, have 30 more vibrational modes among which the energy can be distributed, and have more C_2 units to "evaporate" to reach the structural limit. There may not be enough energy to drive losses to the same termini as observed for the C_{60} complexes within the ~1.5 μs time limit for observable fragmentation.

The ranges of the fragment ion series from the original endohedral precursor ions, $Rg@C_{60}^{•+}$ and $Rg@C_{70}^{•+}$, upon collisional activation show parallel but less pronounced trends compared to the complexes that have captured a He atom (see Table 1). For these series, the size of the internal constituent also plays a role in limiting the extent of fragmentation. The end points are again strong evidence for an endohedral location of the original noble-gas atom. Activated fragmentation from

$C_{60}^{•+}$ and $C_{70}^{•+}$ reaches an absolute limit for closed-structure species of $C_{32}^{•+}$,[17] but we achieved only $C_{36}^{•+}$ from $C_{60}^{•+}$ and $C_{50}^{•+}$ from $C_{70}^{•+}$ in this study. The internal energies that are initially resident in the ions and those available from the collision activation, the kinetic factors for the decompositions, and the dissipation of internal energy by successive C_2 losses or equivalent are likely the limiting factors.

Another trend from Table 1 is that the largest empty species derived from $Rg@C_{60}^{•+}$ are also inversely correlated with increasing size of the endohedral component. This correlation likely reflects a size dependence for getting the endohedral component out of the fullerene. The propensity of $Rg@C_{70}^{•+}$ to give $C_{60}^{•+}$ appears to be driven by the higher stability of $C_{60}^{•+}$.

A final trend is that the relative abundances of the $RgHe@C_{60}^{•+}$ and $RgHe@C_{70}^{•+}$ are positively correlated with the size of the endohedral gas, particularly for the C_{60} case. We cannot attribute this trend to small differences in the available collision energy for the various complexes, because $Ar@C_{60}^{•+}$ would be out of order for such an explanation.

We conclude that tandem mass spectrometry provides a route for the *in situ* preparation and study of endohedral fullerene complexes that contain, in addition to the original noble-gas atom, a He atom that was captured during collision. Evidence for the endohedral location of both the captured He and the original captive noble-gas atom comes from the survival of the capture complexes during transit through the second stage of mass spectrometry (~50 μs) even though they have acquired more than 34 eV of additional internal energy from the capture of He, the retention of both noble-gas atoms during fragmentation, and the existence of end points of the product-ion series that correlate inversely with the size of the internal constituents.

The role of tandem mass spectrometry in demonstrating the existence of endohedral complexes with two noble-gas atoms parallels that in the original demonstration that noble-gas endohedral complexes can be prepared by high-energy collisions of empty fullerene ions and noble-gas targets.

JA971104L